INTERNATIONAL ATOMIC ENERGY AGENCY
UNITED NATIONS EDUCATIONAL, SCIENTIFIC AND CULTURAL ORGANIZATION
INTERNATIONAL CENTRE FOR THEORETICAL PHYSICS
I.C.T.P., P.O. BOX 586, 34100 TRIESTE, ITALY, CABLE: CENTRATOM TRIESTE

H4.SMR/845-4

Second Winter College on Optics

20 February - 10 March 1995

Coherence of Light

F. Gori

University of Rome "La Sapienza"
Department of Physics
Rome, Italy

INTERNATIONAL CENTRE FOR THEORETICAL PHYSICS

SECOND WINTER COLLEGE ON OPTICS

(20 February - 10 March 1995)

COHERENCE OF LIGHT

F.Gori

Department of Physics

University of Rome, "La Sapienza"

P.le A. Moro, 2 - Rome 00185

Italy

1) INTRODUCTION 1

2) AN INTUITIVE INTRODUCTION TO COHERENCE 1
2.1) The speckle model 1
2.2) Time varying speckles and partially coherent fields 5

3) FUNDAMENTALS OF COHERENCE THEORY 10
3.1) Analytic signal 10
3.2) Mutual coherence function 12

4) EVALUATION OF COHERENCE FUNCTIONS 15
4.1) Wiener-Kintchine and van Cittert-Zernike theorems 15
4.2) Examples 16

5) COHERENCE IN THE SPACE-FREQUENCY DOMAIN 20
5.1) Cross spectral density 20
5.2) The modal theory of coherence 22
5.3) An example 25
5.4) Propagation of partially coherent fields 27
5.5) Spectral changes induced by source correlations 31
5.6) A glance at further topics of coherence theory 34

REFERENCES 35

1) INTRODUCTION

The kind of light we normally encounter in everyday life is partially coherent. It is neither strictly predictable like an idealized monochromatic field nor totally disordered. The field fluctuations possess a certain degree of correlation both in time and in space. Strange as it may sound at first, it is precisely this often minute amount of correlation that carries the most important information contained in the light field. In addition, the quantity of information to be found in the field is usually very large. So large, in fact, that even nowadays, in spite of the great advances in optical technology, its practical registration is a challenging task. While you can use holography to freeze and recreate a coherent wavefront passing through remarkably large areas, no one knows how to record and reproduce, in a sensible way, the field coming from ordinary objects (trees, mountains, ...) under the light of sun and passing through a window pane. This is an unsolved problem of contemporary optics.

The theory of partially coherent fields or briefly the coherence theory received its modern formulation through several fundamental papers by E. Wolf. An exposition of these results can be found in ref. 1. Further general readings are refs. 2 and 3. Today, coherence theory includes an impressive amount of knowledge thanks to the works of a large number of authors in the course of some thirty years. The interest in researches dealing with partially coherent fields is far from subsiding and many new results keep appearing in the scientific literature. Of course, we cannot give a complete account of the present state of the theory in these introductory notes. We would like, however, to give the reader some flavour of current researches. To this aim, we choose the following plan. After an intuitive introduction, we shall present a brief summary of the foundations of the theory as well as some of its most traditional applications. We shall then discuss basic elements of more recent developments, notably the space-frequency domain approach. After describing the space frequency domain approach, which is currently used in investigations on coherence theory, we shall concentrate on some propagation phenomena. In particular, we shall discuss how the correlation properties of the source affect the measurement of the spectrum of the radiation field.

2) AN INTUITIVE INTRODUCTION TO COHERENCE

2.1) The speckle model

As well known, most objects under illumination with coherent light such as that produced by a laser give rise to a scattered field exhibiting a granular appearance known as

speckling. Such phenomenon can be interpreted as a random interference among the wavelets coming from different points of the scatterer. To be more specific, let us refer to the scheme of fig. 2.1.1. A ground glass is hit by a laser beam and the transmitted light is observed on a screen S_1 at a distance z from the scatterer. We assume that the diameter, say d, of the laser spot on the glass is much smaller than z. We further assume that the grooves on the glass have a depth much larger than the wavelength, say λ, of the radiation field. Let us divide the surface of the scatterer into tiny areas within which the optical path through the glass may be considered to be constant. The phases of the wavelets emerging from the various areas are randomly distributed between 0 and 2π. In order to obtain a rough estimate of the speckle size, let us consider the wavelets coming from two certain areas. Two such wavelets produce, by themselves, Young fringes. When all the wavelets emerging from the scatterer are simultaneously considered, we can think of the resulting

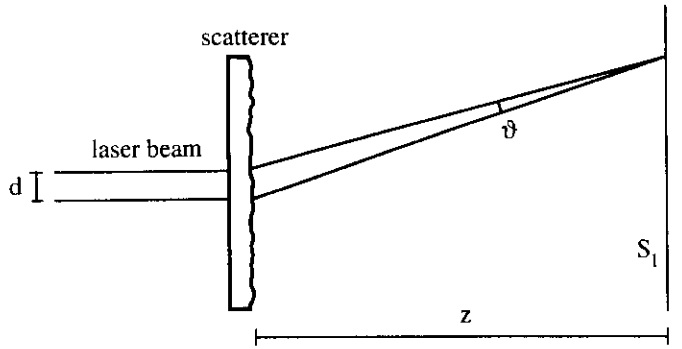

fig. 2.1.1

pattern as a superposition of a large set of Young fringes with various orientations and spacings that further interfere with one another. As a result, speckles appear and we can assume that their width is roughly equal to some mean spacing of the underlying Young fringes. Such a spacing can be estimated by taking two areas at a mutual distance equal to, say, d/2. They give fringes whose width L is (see fig. 2.1.1 for notations)

$$L \cong \frac{\lambda}{\vartheta} \cong \frac{2\lambda z}{d}, \qquad (2.1.1)$$

and this is also an estimate of the speckle size.

Let us refer to an ensemble of realizations of our scattering experiment. At a typical point on S_1 the field behaves as a random, zero mean variable. Use of the central limit theorem suggests that this variable is of the gaussian type. The existence of speckles reveals that such a random variable cannot change too rapidly on the screen. If we consider two

points whose distance is smaller than the speckle size we expect the field values at those points to be highly correlated on an ensemble average. In other words, the mean area of a speckle can be considered as a visualization of the correlation area for the field.

For a more complete description, we introduce the spatial correlation function $C(\mathbf{r}_1, \mathbf{r}_2)$ of the speckle field at two points with radius vectors $\mathbf{r}_1$ and $\mathbf{r}_2$

$$C(\mathbf{r}_1,\mathbf{r}_2) = \langle V(\mathbf{r}_1)V^*(\mathbf{r}_2)\rangle, \qquad (2.1.2)$$

where V is the scalar disturbance describing the spatial part of the monochromatic field. The angular brackets denote an ensemble average and the asterisk stands for complex conjugate. To get rid of trivial factors depending on the overall power of the field, one introduces the following normalized version of the correlation function

$$c(\mathbf{r}_1,\mathbf{r}_2) = \frac{C(\mathbf{r}_1,\mathbf{r}_2)}{\sqrt{C(\mathbf{r}_1,\mathbf{r}_1)C(\mathbf{r}_2,\mathbf{r}_2)}}. \qquad (2.1.3)$$

It will be noted that the functions appearing in the denominator simply give the averaged intensity at the two points, or

$$C(\mathbf{r}_j,\mathbf{r}_j) = \langle |V(\mathbf{r}_j)|^2 \rangle = \langle I_j \rangle, \qquad (j = 1,2). \qquad (2.1.4)$$

The following inequality can be proved

$$0 \le |c(\mathbf{r}_1,\mathbf{r}_2)| \le 1. \qquad (2.1.5)$$

The function c whose modulus can be taken as a measure of the correlation between the disturbances at $\mathbf{r}_1$ and $\mathbf{r}_2$ is termed degree of correlation.

We can evaluate the function C for a geometry of the form illustrated in fig. 2.1.1. Let $V_0(\boldsymbol{\rho})$ be the field distribution across the scatterer plane (see fig. 2.1.2). The field $V_z(\mathbf{r})$ on S_1 can be computed, in the paraxial approximation, through the well known Fresnel integral

$$V_z(\mathbf{r}) = -\frac{ie^{ikz}}{\lambda z}\int V_0(\boldsymbol{\rho}) e^{\frac{ik}{2z}(r-\rho)^2} d^2\rho, \qquad (2.1.6)$$

where $k=2\pi/\lambda$. We write $V_z(\mathbf{r}_1)$ and $V_z^*(\mathbf{r}_2)$ by means of eq. (2.1.6) and average their

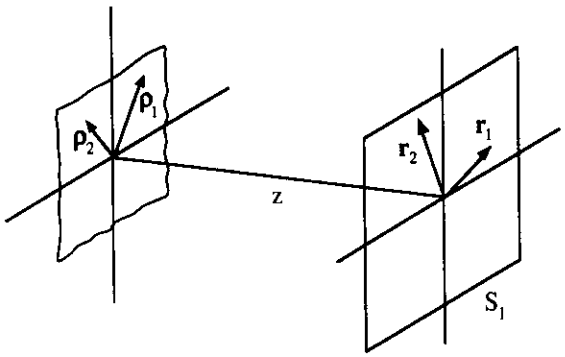

fig. 2.1.2

product. Taking into account eq. (2.1.2), the result can be written

$$C_z(\mathbf{r}_1,\mathbf{r}_2)=\frac{1}{\lambda^2 z^2}\iint C_0(\boldsymbol{\rho}_1,\boldsymbol{\rho}_2)\,e^{\frac{ik}{2z}\left[(\mathbf{r}_1-\boldsymbol{\rho}_1)^2-(\mathbf{r}_2-\boldsymbol{\rho}_2)^2\right]}\,d^2\rho_1 d^2\rho_2\,, \tag{2.1.7}$$

where C_0 and C_z are the correlation functions at the scatterer and the observation plane, respectively. Equation (2.1.7) is the propagation formula for the correlation function. The evaluation of C_z is traced back to that of C_0. The latter, in turn, depends on the features of the scatterer. The simplest case occurs when the tiny areas of the scatterer in which the optical path stays constant have negligible linear dimensions, say of the order of λ. Then, C_0 can be approximated by

$$C_0(\boldsymbol{\rho}_1,\boldsymbol{\rho}_2)=K\langle I_0(\boldsymbol{\rho}_1)\rangle\delta(\boldsymbol{\rho}_2-\boldsymbol{\rho}_1)\,. \tag{2.1.8}$$

where δ is the Dirac function. As well known, when the Dirac δ-function is used to approximate a well behaving function attention must be paid to dimensional factors. In order to obtain dimensionally correct results when eq. (2.1.8) is inserted into eq. (2.1.7), K must have the dimensions of an area. The physical meaning of K is that of the correlation area on the scatterer. According to our previous hypotheses, we set $K=\lambda^2$. As a consequence, eqs. (2.1.7) and (2.1.8) give

$$C_z(\mathbf{r}_1,\mathbf{r}_2)=\frac{e^{\frac{ik}{2z}\left(r_1^2-r_2^2\right)}}{z^2}\int\langle I_0(\boldsymbol{\rho})\rangle\,e^{-\frac{2\pi i}{\lambda z}(\mathbf{r}_1-\mathbf{r}_2)\cdot\boldsymbol{\rho}}\,d^2\rho\,, \tag{2.1.9}$$

where the suffix 1 in $\boldsymbol{\rho}_1$ has been dropped. Apart from the factor in front of the integral, which does not depend on the scatterer, the correlation function C_z is determined by the Fourier transform of the averaged intensity distribution across the scatterer. Note that this Fourier transform is to be evaluated at the spatial frequency $(\mathbf{r}_1-\mathbf{r}_2)/(\lambda z)$, i. e., it depends on $\mathbf{r}_1$ and $\mathbf{r}_2$ only through their difference. It is also worthwhile to observe that the Fourier integral appearing in eq. (2.1.9) is reminiscent of Fraunhofer phenomena. Yet, we only assumed to be in the Fresnel region. The quadratic terms in $\boldsymbol{\rho}_1$ and $\boldsymbol{\rho}_2$ within the exponential in eq. (2.1.7) disappear by virtue of eq. (2.1.8). If the far-zone hypothesis applies, eq. (2.1.9) can be further simplified in that the exponential function in front of the integral can be approximated by one.

As a simple example, we consider the case in which a circular region with diameter d is uniformly illuminated on the scatterer with mean intensity $\langle I_0\rangle$. The integral in eq. (2.1.7) is easily evaluated. Using eq. (2.1.3) we obtain the following degree of correlation

$$c_z(\mathbf{r}_1,\mathbf{r}_2)=e^{\frac{ik}{2z}\left(r_1^2-r_2^2\right)}\frac{2J_1\left(\frac{\pi d}{\lambda z}|\mathbf{r}_1-\mathbf{r}_2|\right)}{\frac{\pi d}{\lambda z}|\mathbf{r}_1-\mathbf{r}_2|}\,, \tag{2.1.10}$$

where J_1 is the Bessel function of the first kind and order one. The first zero of c_z is reached for a certain value of $|\mathbf{r}_1-\mathbf{r}_2|$, say $|\mathbf{r}_1-\mathbf{r}_2|_0$ such that the argument of J_1 is 3.83, or

$$|\mathbf{r}_1-\mathbf{r}_2|_0=\frac{3.83}{\pi}\frac{\lambda z}{d}\,. \tag{2.1.11}$$

This can be taken as the radius of the correlation area in the neighbourhood of a typical point. The corresponding diameter, namely, $2.42\lambda z/d$ is in good agreement with the elementary estimate (2.1.1).

2.2) Time varying speckles and partially coherent fields

Let us refer to the set-up drawn in fig. 2.2.1. The main difference with respect to the case of fig. 2.1.1 is that the scatterer can be changed in time by setting the ground glass into rotatory motion. If the motor rotates at a sufficiently low speed, we shall see the observation screen swarming with changing speckles. On increasing the motor speed our eye will no longer be able to follow the speckle change and the screen will appear uniformly illuminated. We have synthesized a spatially incoherent source, known as a pseudo-thermal source. To a certain extent, this resembles an ordinary extended source such as a glow

discharge lamp. It is to be noted that even if the light falling on the rotating ground glass were perfectly monochromatic the scattered light would have a spectrum with non-zero width because of the random phase modulation introduced by the moving glass. The spectrum width is an increasing function of the motor speed.

Other types of devices could be used for obtaining a similar result. For example, we could use scattering from an assembly of tiny dielectric spheres suspended in a stirred liquid. The above scheme is particularly simple in practice and has the advantage that the

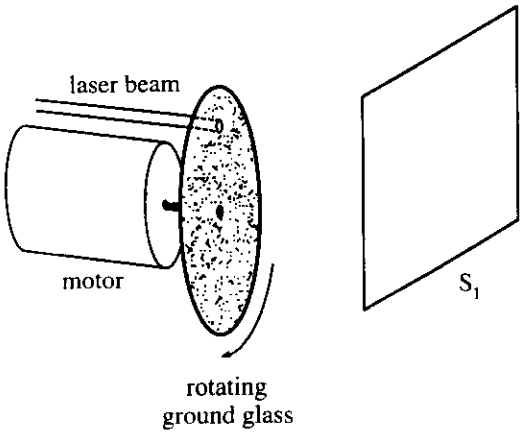

fig. 2.2.1

time evolution of the system can be interrupted simply by stopping the motor. We shall refer to it in the following.

The light emerging from our pseudo-thermal source is partially coherent from both the spatial and the temporal viewpoints. Although we do not see speckles any more, in a sense they are still there. We can think that a sort of rain of three-dimensional speckles falls on the observation screen. Their cross-section represents the so-called coherence area. The values of the field at the same instant for two points within such an area have strongly correlated time fluctuations. The extent of the speckles along z is generally termed the coherence length and the time needed for light to travel this length is known as the coherence time. This means that the field fluctuations at a certain point for two different instants remain highly correlated until the separation between the instants does not exceed the coherence time.

It is important to note the the simple trick of moving the ground glass has considerably changed the primitive process. In our initial considerations, correlation was defined in terms of averages over a suitable ensemble of realizations. Conceptually, time played no role because in principle an arbitrarily high number of replicas of the experiment

could exist simultaneously. Once the scatterer is set into motion, time becomes a key ingredient of the process and we look quite naturally at time rather than ensemble averages. Roughly speaking, we have transformed our initial time independent process into a stationary ergodic process. The new process, however, has some extra richness in that besides spatial correlations temporal correlations were introduced. Of course, the temporal correlation properties depend on the manner in which the time evolution is realized. For the simple device of fig. 2.2.1, the coherence time is a decreasing function of the motor speed.

How can the correlation properties be put into evidence experimentally? Let us start from the spatial correlations. We stop the motor and make two pinholes on the screen S_1.

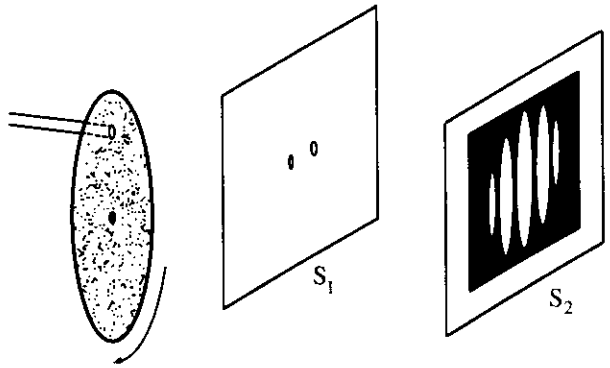

fig. 2.2.2

Then, we collect the light emerging from the pinholes on a second screen S_2 (fig. 2.2.2) whose distance from S_1 is large with respect to the pinhole separation. We first assume that the pinhole separation is smaller than the speckle size. As a consequence, the field values of the two pinholes have only slight differences in amplitude and phase. Good Young fringes will be seen on S_2 although occasionally they can be very dim if the pinholes happen to be in a dark region of the speckle pattern. Now, move the ground glass and stop it at a different position. Again, good fringes will appear on S_2. Even if the amplitude and phase of the field at each pinhole can vary considerably with respect to the previous case, the amplitude and phase differences of the field values at the two pinholes remain small. Accordingly, the contrast and the position of the fringes will be nearly identical to that of the previous pattern. Therefore, when the ground glass is set into a continuos and fast motion good fringes will survive on S_2 under time average. Although we do not see speckles on S_1 any longer, the existence of a coherence area is revealed by the presence of the fringes.

We can now repeat the experiment with a pair of pinholes whose separation is much greater than the speckle size. For each still position of the ground glass we can see fringes. However, passing from one position to another the fringes change. Sometimes, one of the

pinholes is located in a dark region while the other one is well lit. The fringes are scarcely contrasted. Some other times, both pinholes are equally illuminated and good fringes appear. In certain cases, the fields at the pinholes are in phase and a bright fringe appears at the center of the pattern. In other cases, they are in antiphase and each bright fringe is replaced by a dark one. When the motor is powered up, all these different fringe systems wash out and we do not see any interference effect (on time average). The fields at the pinholes are incoherent. In conclusion, we can assess the spatial coherence properties using a set-up à la Young interferometer.

In order to see the effects of the temporal correlations we refer to the set-up of fig.2.2.3. There is only one pinhole on S_1. Light emerging from the pinhole is collimated by a

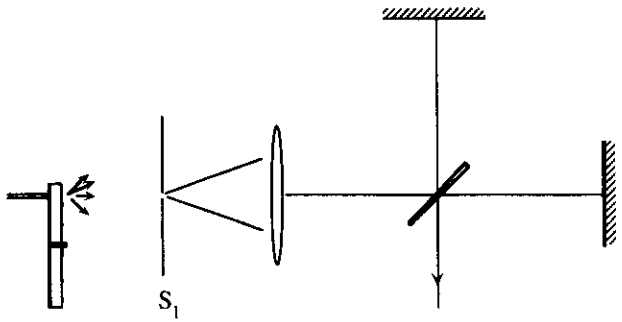

fig. 2.2.3

converging lens and the resulting beam is fed into a Michelson interferometer. Because of the change of the speckle pattern on S_1, the beam is temporally modulated. We can think of it as a sequence of wavetrains. Within each wavetrain the field behaves as an approximately sinusoidal signal whereas passing from one wavetrain to another random variations of amplitude and phase occur. At the entrance beam-splitter, each wavetrain is divided into two copies that go along the two arms. Suppose the path difference between the two arms is small in comparison with the wavetrain length. At the output of the interferometer, each copy of the wavetrains overlap with its twin. In this case, the fringe position on an observation screen depends only on the geometry of the interferometer and does not change from one wavetrain to the other although the fringe brightness can vary. On time average, good fringes are seen. Suppose now that the path difference between the two arms is increased until it becomes larger than the wavetrain length. Copies originated from different wavetrains overlap at the output. The resulting fringes vary both in contrast and in position because of the random changes of the field amplitude and phase when one input wavetrain is replaced by the next one. On time average, the fringe pattern cancels out. From a practical point of view, the path difference to be introduced between the interferometer arms may be

very large because the length of the wavetrains produced by our apparatus is considerable but this is conceptually immaterial.

The same interferometers can be used with light generated by an ordinary source. Let us consider an extended thermal source, e.g., an incandescent body. We put in front of it a narrowband filter (fig.2.2.4). Let $\Delta\nu$ be the allowed frequency band centered at some mean frequency ν_o ($\nu_o >> \Delta\nu$). What shall we see on the observation screen S_1? At any time the source can be thought of as an assembly of independent pointlike radiators emitting nearly monochromatic spherical waves with bandwidth $\Delta\nu$ whose amplitudes and phases are randomly distributed. For a time span much smaller than $1/\Delta\nu$, the amplitude and phase of each wave remains nearly constant. As a consequence, we expect speckles to be formed across S_1. We further expect the speckles to change as time goes on and becomes greater than $1/\Delta\nu$. To a certain extent, this picture can be adopted even if the filter is removed. In this case, $\Delta\nu$ becomes the bandwidth of the complete spectrum emitted by the source.

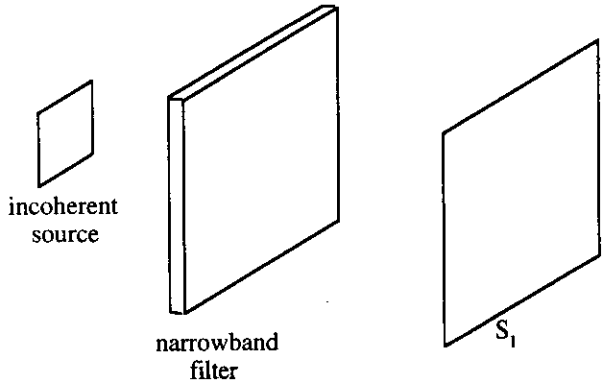

fig. 2.2.4

In the course of time, a crowd of coherence cigars, so to say, fall on the screen S_1. Each of them has a cross-section equal to the coherence area and a longitudinal extent equal to the coherence length. This is how we picture the light field arriving on the observation screen. Is such a picture correct? Could we record the speckle pattern that should be seen on S_1 in a sufficiently small time? Let us start by the second question. For a spectral lamp such as a rare gas glow discharge the emitted spectrum is made up of separated lines. A typical line, which can be isolated by means of a suitable filter, has a coherence length of the order of 10 cm, or equivalently, a coherence time of the order of some tenths of one nanosecond. We should make our observation on a time interval smaller than this. This is not easy but could be done. The main problem, however, is that with ordinary sources we could hardly record anything on, say, a photographic emulsion after so short an exposure. As a matter of fact, one finds that an ordinary thermal source distributes the energy of one photon among some

10^3-10^4 coherence cigars. Hence, there is not enough energy to record a speckle pattern in a time interval shorter than the coherence time. Does this mean that our model is incorrect? Well, it is correct in classical terms. Nevertheless, when quantization is taken into account the optical intensity in a coherence cigar is to be thought of as proportional to the probability of finding a photon. Although the above difficulty does not prevent the use of our model in the classical theory, it makes practically impossible certain experiments. This is why many experiments on coherence theory are performed using pseudo-thermal sources where, thanks to the extremely high power emitted by lasers per unit bandwidth, such a difficulty does not occur.

3) FUNDAMENTALS OF COHERENCE THEORY

3.1) Analytic signal

After our introduction to an intuitive understanding of basic quantities of coherence theory, we want to describe in analytical terms the foundations of coherence theory.

Preliminarily, we need to recall the standard way in which the complex formalism, well known for monochromatic signals, can be extended to the polychromatic case. Let U(P,t) be the real disturbance describing our field. We assume that it admits a Fourier representation of the form

$$U(P,t) = \int_{-\infty}^{\infty} u(P,\nu) e^{-2\pi i \nu t} d\nu . \qquad (3.1.1)$$

In order to extend the complex formalism, we proceed in much the same way as with sinusoidal signals. In that case, we associate to the real function $\cos(2\pi\nu t) = [\exp(2\pi i\nu t)+\exp(-2\pi i\nu t)]/2$ the complex representation $\exp(-2\pi i\nu t)$. This is equivalent to suppress the negative frequency term $\exp[-2\pi i(-\nu)t]$ and to double the other one. Doing the same for the polychromatic signal, leads to the so-called analytic signal, namely,

$$V(P,t) = 2\int_{0}^{\infty} u(P,\nu) e^{-2\pi i \nu t} d\nu . \qquad (3.1.2)$$

We denote it by the same symbol V that was previously used for the spatial part of a monochromatic field. Now, however, V is a function of both space and time. The analytic signal can be given the form

$$V(P,t) = A(P,t)\, e^{-2\pi i \nu_0 t + i\Phi(P,t)} , \qquad (3.1.3)$$

where A e Φ are real functions termed amplitude and phase respectively, and ν_0 is some mean frequency of the field. Although valid for any field, expression (3.1.3) is particularly meaningful for the so-called quasi-monochromatic case. This means that the function u(P,ν) is appreciably different from zero only in a frequency interval $\Delta\nu$ that is small with respect to the mean frequency ν_0. In that case, A and Φ are slowly variable with respect to $1/\nu_0$ as we shall see in a moment. On equating the right hand sides of eqs. (3.1.2) and (3.1.3) we obtain

$$A(P,t)\, e^{i\Phi(P,t)} = \int_{0}^{\infty} u(P,\nu) e^{-2\pi i(\nu-\nu_0)t} d\nu . \qquad (3.1.4)$$

In particular, for t=0 we have

$$A(P,0)\, e^{i\Phi(P,0)} = \int_{0}^{\infty} u(P,\nu)\, d\nu . \qquad (3.1.5)$$

Note that the integrals in eqs. (3.1.4) and (3.1.5) remain nearly equal to each other until the exponential $\exp[-2\pi i(\nu-\nu_0)t]$ is almost unity for all frequencies at which u(P,ν) is significantly different from zero. By virtue of the quasi-monochromaticity hypothesis [u(P,ν) vanishing outside a band $\Delta\nu$ centered at ν_0], this holds true for all values of t satisfying the condition

$$t\,\Delta\nu << 1 . \qquad (3.1.6)$$

Therefore, A(P,t) e Φ(P,t) can be significantly different from A(P,0) e Φ(P,0) only when t is large enough to violate condition (3.1.6), say when t becomes of the order of

$$t \cong \frac{1}{\Delta\nu} , \qquad (3.1.7)$$

or greater than that. Because of the previous hypotheses ($\Delta\nu << \nu_0$), we have

$$t \cong \frac{1}{\Delta\nu} >> \frac{1}{\nu_0} . \qquad (3.1.8)$$

In conclusion, in the quasi-monochromatic case the analytic signal written as in eq. (3.1.3) takes on the form of a monochromatic signal undergoing a slow amplitude and phase modulation.

3.2) Mutual coherence function

Let us consider two points P_1 and P_2 in the wavefield and two instants t_1 and t_2. The mutual coherence function of the field at $(P_1, t_1,)$ and (P_2,t_2) is defined as(+)

$$\Gamma(P_1,t_1;P_2,t_2) = \left\langle V(P_1,t_1)V^*(P_2,t_2)\right\rangle , \qquad (3.2.1)$$

where the angular brackets denote ensemble average. In most cases of interest the stochastic process associated to V is stationary and ergodic. Then Γ depends on t_1 and t_2 only through their difference $\tau = t_1 - t_2$ and the ensemble average can be replaced by a time average. Accordingly, we shall refer to the mutual coherence function in the form

$$\Gamma_{12}(\tau) = \left\langle V_1(t+\tau)V_2^*(t)\right\rangle , \qquad (3.2.2)$$

where obvious shorthand notations are used and the average is meant to be over time.

In particular, for $P_1 = P_2$ and $\tau = 0$, eq. (3.2.2) gives the mean intensity

$$\Gamma_{jj}(0) = I_j , \qquad (j = 1,2) , \qquad (3.2.3)$$

where, according to the usual conventions of coherence theory, the average sign on I is omitted.

The normalized version of eq. (3.2.2) reads

$$\gamma_{12}(\tau) = \frac{\Gamma_{12}(\tau)}{\sqrt{\Gamma_{11}(0)\Gamma_{22}(0)}} , \qquad (3.2.4)$$

and is known as the complex degree of coherence. The following inequality can be proved

$$0 \le |\gamma_{12}(\tau)| \le 1 . \qquad (3.2.5)$$

The function $\Gamma_{12}(t)$ [or $\gamma_{12}(\tau)$] takes simultaneously into account both spatial and temporal correlations. In order to divide their roles, it is said that $\Gamma_{12}(0)$ describes the spatial

(+) An alternative form given by the complex conjugate of eq. (3.2.1) is also used.

coherence of the field whereas $\Gamma_{jj}(\tau)$,, (j = 1,2) describes the temporal coherence. A sharper distinction between space and time coherence will be seen later.

A field is said to be completely coherent if $|\gamma_{12}(\tau)| = 1$ for any choice of P_1, P_2 and τ. This occurs in the case of a strictly monochromatic field no matter how complicated is the spatial structure. For example, the field coming from a static scatterer under monochromatic illumination is perfectly coherent in spite of the speckle phenomenon. This is due to the fact that the temporal evolution of the field is completely predictable.

The other limiting case, namely, complete incoherence, would require $|\gamma_{12}(\tau)| = 0$ for any choice of P_1, P_2 and τ, except for $P_1 = P_2$ and $\tau = 0$. An actual radiation field is neither completely coherent nor completely incoherent. Rather, it is partially coherent. This means that at any point P_1 we have $|\gamma_{11}(\tau)| \simeq 1$ until τ does not exceed a certain value Δt_c known as coherence time. On the ground of the results of section 3.1 we can anticipate that

$$\Delta t_c \cong \frac{1}{\Delta\nu} , \qquad (3.2.6)$$

where $\Delta\nu$ is the bandwidth of the field. A more complete description will be seen in the next section. Similarly, in the neighbourhood of P_1 there is a set of points P_2, forming the so-called coherence are, such that $|\gamma_{12}(0)| \simeq 1$. Roughly speaking, the linear dimensions of the coherence area can be evaluated through eq.(2.1.1) by using the mean wavelength of the radiation field. We shall come back to this point is the next section.

The case of quasi-monochromatic fields ($\Delta\nu << \nu_o$) is of utmost importance. In this case, for any delay τ obeying the condition

$$\tau << \frac{1}{\Delta\nu} \cong \Delta t_c , \qquad (3.2.7)$$

the following approximation holds

$$\Gamma_{12}(\tau) \cong \Gamma_{12}(0)e^{-2\pi i\nu_o\tau} . \qquad (3.2.8)$$

Within the range of values of τ such that eq. (3.2.2) is satisfied, the coherence properties are determined by $\Gamma_{12}(0)$. The function

$$J(P_1, P_2) = J_{12} = \Gamma_{12}(0) , \qquad (3.2.9)$$

is called the mutual intensity. Its normalized version

$$\mu(P_1, P_2) = \mu_{12} = \gamma_{12}(0)\,, \tag{3.2.10}$$

retains the name of complex degree of coherence.

For quasi-monochromatic fields propagation phenomena can be described by means of the mutual intensity because propagation formulas for J_{12} exist. Here, we shall limit ourselves to the paraxial propagation case in which the propagation formula is the same as that relating to the speckle correlation function (2.1.7), namely,

$$J(\mathbf{r}_1,\mathbf{r}_2) = \frac{1}{\lambda_o^2 z^2}\iint J_o(\boldsymbol{\rho}_1,\boldsymbol{\rho}_2)\, e^{\frac{ik}{2z}\left[(r_1-\rho_1)^2-(r_2-\rho_2)^2\right]}\, d^2\rho_1 d^2\rho_2\,, \tag{3.2.11}$$

where λ_o is the mean wavelength and $k_o=2\pi/\lambda_o$. Notations for the geometrical quantities of eq.(3.2.11) are the same as in fig. 2.1.2. Knowledge of the mutual intensity J_o across the integration plane permits one to evaluate the mutual intensity J at any pair of points $\mathbf{r}_1$ and $\mathbf{r}_2$ on a plane at a distance z. In particular, for $\mathbf{r}_1=\mathbf{r}_2=\mathbf{r}$, the intensity distribution $I(\mathbf{r})$ can be found by means of the formula

$$I(\mathbf{r}) = \frac{1}{\lambda_o^2 z^2}\iint J_o(\boldsymbol{\rho}_1,\boldsymbol{\rho}_2)\, e^{\frac{ik}{2z}\left[\rho_1^2-\rho_2^2-2\mathbf{r}\cdot(\boldsymbol{\rho}_1-\boldsymbol{\rho}_2)\right]}\, d^2\rho_1 d^2\rho_2\,. \tag{3.2.12}$$

It will be noted that unlike the coherent case in which knowledge of the two-dimensional field distribution across the first plane would suffice for finding the intensity at any point on the second one, here we need knowledge of the four-dimensional function $J_o(\boldsymbol{\rho}_1,\boldsymbol{\rho}_2)$.

The mutual intensity can be found experimentally through a simple Young interferometer such as the one depicted in fig. 2.2.2. At a typical point on S_2 with position vector $\mathbf{r}$ the intensity can be computed by eq. (3.2.12). If the pinhole area, say S, is negligibly small, we can approximate the result by

$$I(\mathbf{r}) = \frac{S^2}{\lambda_o^2 z^2}\left[I_o(\boldsymbol{\rho}_1)+I_o(\boldsymbol{\rho}_2)+2\,\mathrm{Re}\left\{J_o(\boldsymbol{\rho}_1,\boldsymbol{\rho}_2)\, e^{\frac{ik_o}{2z}\left[\rho_1^2-\rho_2^2-2\mathbf{r}\cdot(\boldsymbol{\rho}_1-\boldsymbol{\rho}_2)\right]}\right\}\right], \tag{3.2.13}$$

where $\boldsymbol{\rho}_1$ and $\boldsymbol{\rho}_2$ are the pinhole position vectors and Re stands for the real part. We use the normalized version of J_o and se

$$e^{\frac{ik_o}{2z}\left(\rho_1^2-\rho_2^2\right)} = e^{i\alpha_{12}}\,, \qquad \mu_o(\boldsymbol{\rho}_1,\boldsymbol{\rho}_2) = \left|\mu_o(\boldsymbol{\rho}_1,\boldsymbol{\rho}_2)\right| e^{i\gamma_{12}}\,. \tag{3.2.14}$$

Then, eq. (3.2.13) becomes

$$I(\mathbf{r}) = \frac{S^2}{\lambda_o^2 z^2}\left\{I_o(\boldsymbol{\rho}_1)+I_o(\boldsymbol{\rho}_2)+ 2\sqrt{I_o(\boldsymbol{\rho}_1)I_o(\boldsymbol{\rho}_2)}\left|\mu_o(\boldsymbol{\rho}_1,\boldsymbol{\rho}_2)\right|\cos\left[\alpha_{12}+\gamma_{12}-\frac{k_o}{z}\mathbf{r}\cdot(\boldsymbol{\rho}_1-\boldsymbol{\rho}_2)\right]\right\}. \tag{3.2.15}$$

The interference term in eq. (3.2.15) has a weight proportional to $|\mu_o|$. In addition, the origin of the fringe system depends on γ_{12}. Therefore examination of the fringe pattern can furnish the degree of coherence at $\boldsymbol{\rho}_1$ and $\boldsymbol{\rho}_2$. It is customary to describe the contrast of the fringes by means of the so-called visibility defined as

$$\mathcal{V} = \frac{I_{Max}-I_{min}}{I_{Max}+I_{min}}\,. \tag{3.2.16}$$

where I_{Max} and I_{min} are the maximum and minimum intensity values in the neighbourhood of the observation point. Use of eq. (3.2.15) leads to

$$\mathcal{V} = \frac{2\sqrt{I_o(\boldsymbol{\rho}_1)I_o(\boldsymbol{\rho}_2)}}{I_o(\boldsymbol{\rho}_1)+I_o(\boldsymbol{\rho}_2)}\left|\mu_o(\boldsymbol{\rho}_1,\boldsymbol{\rho}_2)\right|. \tag{3.2.17}$$

In particular, if $I_o(\boldsymbol{\rho}_1)=I_o(\boldsymbol{\rho}_2)$ eq. (3.2.17) becomes

$$\mathcal{V} = \left|\mu_o(\boldsymbol{\rho}_1,\boldsymbol{\rho}_2)\right|. \tag{3.2.18}$$

4) EVALUATION OF COHERENCE FUNCTIONS

4.1) Wiener-Kintchine and van Cittert-Zernike theorems

We repeatedly used the fact that the coherence time is roughly proportional to the inverse of the bandwidth of the field. Actually, the spectrum of the field completely specifies the temporal coherence properties. In fact, a celebrated theorem, namely, the Wiener-Kintchine theorem asserts that

$$\Gamma_{11}(\tau) = \int_0^\infty G_{11}(\nu)\, e^{-2\pi i\nu\tau}\, d\nu\,, \tag{4.1.1}$$

where $G_{11}(\nu)$ is the spectral density (on power spectrum) at the observation point. The lower limit in the integral is zero because the analytic signal has no negative frequency components. At first, it might seem that specification of the observation point is unnecessary. This is not so because, in the general case, the spectral density does depend on the observation point. We shall discuss this point later on.

There is a counterpart of the Wiener-Kintchine theorem in the spatial domain. This is the van Cittert-Zernike theorem that applies to spatially incoherent quasi-monochromatic planar sources. Then, the mutual intensity across the source can be approximated by

$$J_0(\boldsymbol{\rho}_1,\boldsymbol{\rho}_2) = \lambda_0^2 I_0(\boldsymbol{\rho}_1)\delta(\boldsymbol{\rho}_2-\boldsymbol{\rho}_1), \tag{4.1.2}$$

where $\boldsymbol{\rho}_1$ and $\boldsymbol{\rho}_2$ are position vectors in the source plane. The similarity between eqs.(2.1.8) and (4.1.2) will be noted. We only consider the paraxial form of the theorem. In this case, for two points specified by the position vectors $\mathbf{r}_1$ and $\mathbf{r}_2$ in a plane parallel to the source plane at a distance z, the van Cittert-Zernike theorem reads

$$J(\mathbf{r}_1,\mathbf{r}_2) = \frac{e^{\frac{ik}{2z}(r_1^2-r_2^2)}}{z^2}\int I_0(\boldsymbol{\rho})\, e^{-\frac{2\pi i}{\lambda z}(\mathbf{r}_1-\mathbf{r}_2)\cdot\boldsymbol{\rho}}\, d^2\rho . \tag{4.1.3}$$

as can be seen by inserting eq.(4.1.2) into eq.(3.2.11). Again, it will be noted that this result is substantially identical to the formula (2.1.9) relating to the speckle correlation function.

We shall work out some examples of application of the present theorems in the next section.

4.2) Examples

The Fourier transform relationship between the spectral density and the temporal coherence function $\Gamma_{11}(\tau)$ furnished by eq.(4.1.1) suggests that, conversely, by measuring Γ_{11} as a function of τ we can obtain the spectral density. This is the idea underlying the fluorishing technique known as Fourier spectroscopy [4]. To give an idea of this technique, we refer to the scheme of fig. 4.2.1. Light from the source of interest, after collimation, is fed into a Michelson interferometer. For the sake of clarify, counterpropagating beams are drawn with separated lines. Disregarding the beams 1''' and 2''' that come back to the source, beams 1'' and 2'' provide on the output screen S two superimposed copies of the input with a mutual time delay determined by the lengths of the interferometer arms. The compensating plate C made by the same material as the beam-splitter BS insures that the

time delay is the same for any frequency component regardless of the material dispersion properties.

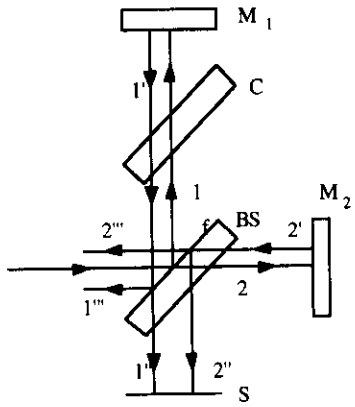

fig. 4

fig. 4.2.1

In the case of perfect collimation of the beams and ideal alignment of the interferometer, the output disturbance can be written

$$V_{out}(t) = \alpha\left[V(t-t_1)+V(t-t_2)\right], \tag{4.2.1}$$

where α is a proportionality factor that depends on the reflectivity of BS (mirrors M_1 and M_2 are assumed to be perfectly reflecting while C is assumed to be coated with anti-reflective layers). The output intensity is

$$I_{out} = |\alpha|^2\left[\left\langle |V(t-t_1)|^2\right\rangle + \left\langle |V(t-t_2)|^2\right\rangle + 2\,\mathrm{Re}\left\{\left\langle V(t-t_1)V^*(t-t_2)\right\rangle\right\}\right]. \tag{4.2.2}$$

Because of the stationarity of the field, eq.(4.2.2) can be written

$$I_{out} = 2|\alpha|^2\left[I+\mathrm{Re}\{\Gamma(\tau)\}\right], \tag{4.2.3}$$

where I is the input intensity. Measuring I and I_{out} we can evaluate $\mathrm{Re}\{\Gamma(\tau)\}$. In order to invert eq.(4.1.1) we should know $\Gamma(\tau)$, not only its real part. However, it is easily seen that

$$\int_{-\infty}^{\infty} \mathrm{Re}\{\Gamma(\tau)\}\, e^{2\pi i \nu \tau}\, d\tau = \frac{1}{2}[G(\nu)+G(-\nu)]. \qquad (4.2.4)$$

Accordingly, inverse Fourier transformation of $\mathrm{Re}\{\Gamma(\tau)\}$ leads to a symmetrized version of $G(\nu)$. This does not give rise to any ambiguity in that $G(\nu)$ has no negative frequency component. Of course, $\mathrm{Re}\{\Gamma(\tau)\}$ can be measured up to some maximum value of τ, say τ_M. Equation (4.2.4) is then replaced by

$$\int_{-\tau_M}^{\tau_M} \mathrm{Re}\{\Gamma(\tau)\}\, e^{2\pi i \nu \tau}\, d\tau = \tau_M \,\mathrm{sinc}\,(2\tau_M \nu) * [G(\nu)+G(-\nu)]. \qquad (4.2.5)$$

Here, the well known convolution theorem for Fourier transform has been applied [convolution is denoted by the asterisk and $\mathrm{sinc}(\nu)=\sin(\pi\nu)/(\pi\nu)$]. As seen from eq.(4.2.5), we recover a smoothed version of the spectrum. This will determine the resolving power of the method.

Next, let us briefly discuss an application of the van Cittert-Zernike theorem. Even large telescopes cannot give a resolved image of certain stellar objects. This occurs when the diffraction pattern produced by the finite aperture of the telescope is larger than the extent of the geometrical image of the star. An equivalent way to express the same condition is to say that the coherence area of the light coming from the star exceeds the diameter of the objective so that the incoming field becomes indistinguishable from a plane wave. It is nonetheless possible to measure the angular diameter of the star without resorting to a larger telescope by using the Michelson stellar interferometer depicted in fig. 4.2.2. Substantially, this device makes two small portions of the wavefront interfere in a Young-like manner. These portions are collected by the outer mirrors M_1 and M'_1 whose distance $|\mathbf{r}_1-\mathbf{r}_2|$ can be varied. The resulting beams are led to interfere on the observation screen S by means of auxiliary mirrors M_2 and M'_2 and simple optics. Assuming the star to be equivalent to a uniform disc with diameter d at a distance z, application of the van Cittert-Zernike theorem gives for the degree of coherence

$$\mu(\mathbf{r}_1,\mathbf{r}_2) = \frac{2J_1\left(\frac{\pi d}{\lambda_0 z}|\mathbf{r}_1-\mathbf{r}_2|\right)}{\frac{\pi d}{\lambda_0 z}|\mathbf{r}_1-\mathbf{r}_2|}, \qquad (4.2.6)$$

i. e., the same expression as that seen in eq. (2.1.10) for the degree of correlation of a speckle pattern produced by a uniformly illuminated circular scatterer except that the far-field

approximation applies. In order to evaluate the angular diameter d/z it is enough to find experimentally the value $|\mathbf{r}_1-\mathbf{r}_2|_0$ where the first zero

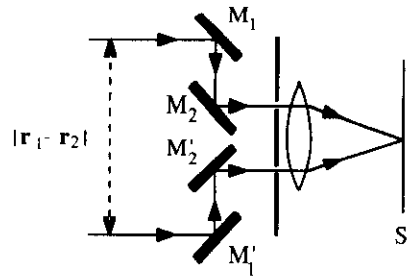

fig. 4.2.2

of μ is reached and the fringes disappear. It follows in fact from eq. (2.1.11)

$$\frac{z}{d} = \frac{\pi}{3.83}\frac{|\mathbf{r}_1-\mathbf{r}_2|_0}{\lambda_0}. \qquad (4.2.7)$$

The maximum value of $|\mathbf{r}_1-\mathbf{r}_2|_0$ that can be detected is about 10 m. For larger distances between the outer mirrors both atmospheric turbulence and mechanical vibrations make the fringe disappear before the zero of μ is reached.

In order to circumvent the above limitations Hanbury Brown and Twiss invented a different device [5]. Suppose the outer mirrors are replaced by photodetectors whose output signals are sent to an electronic correlator. Then, the correlation function for the instantaneous intensities at M_1 and M_2 can be measured. It turns out that such a correlation function can be expressed, for light from ordinary sources, by means of μ_{12}. Therefore, the zeroes of μ_{12} can be found by measurement of the intensity correlation. The influence of phase changes produced by turbulence and mechanical vibrations is eliminated inasmuch as the intensities are measured. As a consequence, much larger values of $|\mathbf{r}_1-\mathbf{r}_2|$ can be used. From the historical point of view the importance of the Hanbury Brown and Twiss interferometer lies in the fact that it gave rise to the study of higher order correlation functions and stimulated the birth of the quantum theory of coherence [2].

The van Cittert-Zermike theorem has an important role in many astronomical applications [6]. As for optics, the applications are countless.

5) COHERENCE IN THE SPACE-FREQUENCY DOMAIN

5.1) Cross spectral density

As we already noticed, the mutual coherence function $\Gamma_{12}(\tau)$ takes simultaneously into account both the spatial and the temporal correlation properties of a field. The division between spatial and temporal aspects was traditionally done along the lines discussed in section 3.2. In particular, spatial coherence is described by $\Gamma_{12}(0)$, i. e., the mutual intensity, whenever the time delays introduced by the apparatus are small with respect to the coherence time. Such a description is not entirely satisfactory as can be seen by a simple example. Let us refer to the experimental set-up of fig. 5.1.1. A pair of partially reflecting

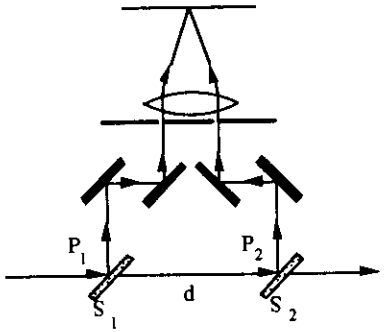

fig. 5.1.1

mirrors S_1 and S_2 are situated at P_1 and P_2 along the path of a plane wave at a distance d from one another. The beams obtained in this way enter an interferometer of the same form examined in section 4.2. The visibility of the fringes on the output plane depend on $\Gamma(P_1,P_2,0)$ because no time delay is introduced by the interferometer. Accordingly, we should say that our experiment gives information about the spatial coherence of the field. However, a moment's thought reveals that in order to assess the output fringes we should compare d with the coherence length of the field. In other words, we are inquiring on time coherence. The reason why such a paradoxical result occurs is that in most considerations about coherence area one implicitly assumes that the line joining P_1 and P_2 is orthogonal to the mean direction of propagation of the radiation. Even if we add such a specification, space and time coherence in the approach based on $\Gamma_{12}(\tau)$ remain intertwined.

It is also important to note that in problems involving the interaction of light with matter frequency-dependent rather than time-dependent response function are used. Correspondingly, it seems appropriate to introduce a space-frequency description of the field correlations.

A satisfactory solution is to introduce the so-called cross spectral density $W(P_1,P_2,\nu)$ [7] defined as

$$W(P_1,P_2,\nu) = \int_{-\infty}^{\infty} \Gamma(P_1,P_2,\tau) e^{2\pi i \nu \tau} d\tau . \qquad (5.1.1)$$

It is seen that the cross spectral density arises from a spectral decomposition of $\Gamma_{12}(\tau)$. The latter is thought of as a superposition

$$\Gamma(P_1,P_2,\tau) = \int_0^{\infty} W(P_1,P_2,\nu)\, e^{-2\pi i \nu \tau}\, d\nu , \qquad (5.1.2)$$

of monochromatic components. Obviously, for $P_1=P_2$, the cross spectral density reduces to the ordinary spectral density, say G(P, ν). It is to be said that the spectral density can play different roles depending on the problem we are considering. In certain cases the frequency is fixed and one is interested in the distribution of the spectral density in space (for example in diffraction and interference phenomena). Then the spectral density is considered as a function of position only and is often termed the optical intensity at the prescribed frequency. In other cases one is interested in the dependence on ν of G. Sometimes the space dependence can be trivial and one speaks of the spectral density without even specifying the observation point. Indeed this was assumed to hold in the discussion of Fourier spectroscopy. Nonetheless, as we shall see later such an independence of G from the space variable does not hold in general and a more accurate discussion is required.

It can be said that $W_{12}(\nu)$ describes the spatial coherence properties because it does not contain the time delay τ. . Its dependence on ν shows that these properties can vary with the frequency. A normalized version of $W_{12}(\nu)$ is obtained as follows

$$\mu(P_1,P_2,\nu) = \frac{W(P_1,P_2,\nu)}{\sqrt{G(P_1,\nu)\, G(P_2,\nu)}} . \qquad (5.1.3)$$

The function μ is called the degree of spatial coherence or the degree of spectral coherence. Its modulus can be proved to satisfy the inequality

$$0 \le |\mu(P_1,P_2,\nu)| \le 1 . \qquad (5.1.4)$$

There is an important point to be made. At first, one might think that $W_{12}(\nu)$ has the following meaning: isolate the monochromatic field component of frequency ν at both P_1 and P_2; then $W_{12}(\nu)$ gives the correlation of these monochromatic fields. This is incorrect. A single monochromatic component is necessarily endowed with perfect coherence (see section 3.2). In particular, the modulus of μ would be one at any frequency. The origin of this difficulty is that for stationary fields the Fourier transform is to be computed by a suitable limiting procedure. On examining this problem, one finds out that the monochromatic component of the field at any fixed frequency ν, actually changes from one realization of the field to another. The value of $W_{12}(\nu)$ is recovered from an ensemble average of the correlation between monochromatic field components (all at frequency ν) in different realizations. The paradox disappears. Although perfect coherence is exhibited in each realization, the amplitude and phase of the correlation function changes across the members of the ensemble. Nevertheless, the mathematical formalism involved in this type of explanation is rather cumbersome and unclear. The picture has been greatly simplified by the modal theory of coherence devised by Wolf [8,9], which we shall outline in the next section.

Before ending this section, we add that propagation formulas for the cross spectral density can be established. In the paraxial approximation, eq. (3.2.11) holds with the mutual intensity J replaced by the cross spectral density W.

5.2) The modal theory of coherence

Let us consider the cross spectral density across a certain plane where a partially coherent field exists. This plane can be thought of as a (primary or secondary) source. We write the following Fredholm homogeneous integral equation of the second kind

$$\int_S W(\mathbf{r}_1,\mathbf{r}_2)\Phi(\mathbf{r}_2)d^2r_2 = \eta\Phi(\mathbf{r}_1)\,, \tag{5.2.1}$$

where $\mathbf{r}_1$ and $\mathbf{r}_2$ are position vectors in the source plane and S is the source area (possibly infinite). The explicit dependence on ν has been dropped. It is reasonable to admit that for physically realizable fields the condition is met that

$$\int_S\int_S \left|W(\mathbf{r}_1,\mathbf{r}_2)\right|^2 d^2r_1 d^2r_2 < +\infty\,, \tag{5.2.2}$$

or, which is the same, that W belongs to the class of Hilbert-Schmidt kernels. Starting from eq. (5.1.1), it can be seen that W is a Hermitian kernel. Furthermore, it is possible to prove

that the kernel is positive. Thanks to these properties, the following conclusions can be drawn. There exists a discrete set of orthonormal eigenfunctions $\Phi_n(\mathbf{r})$, (n=0,1,...) such that

$$\int_S \Phi_n(\mathbf{r})\Phi_m^*(\mathbf{r})d^2r = \delta_{nm}\,, \tag{5.2.3}$$

where δ_{nm} is the Kronecker symbol. The corresponding eigenvalues η_n are real non-negative. In addition, Mercer's theorem can be applied

$$W(\mathbf{r}_1,\mathbf{r}_2) = \sum_{n=0}^{\infty} \eta_n \Phi_n(\mathbf{r}_1)\Phi_n^*(\mathbf{r}_2)\,. \tag{5.2.4}$$

It is in fact eq. (5.2.4) that affords an alternative interpretation of the cross spectral density. To this end, we introduce the ensemble of monochromatic fields

$$\Psi_n(\mathbf{r},t) = \Phi_n(\mathbf{r})e^{-2\pi i\nu t}\,, \qquad (n = 0,1,.....)\,, \tag{5.2.5}$$

and we make a superposition of them of the form

$$U(\mathbf{r},t) = \sum_{n=0}^{\infty} c_n\Psi_n(\mathbf{r},t) = e^{-2\pi i\nu t}\sum_{n=0}^{\infty} c_n\Phi_n(\mathbf{r})\,, \tag{5.2.6}$$

where the c_n are random coefficients. Suppose now that we have an ensemble of realizations of the field (5.2.6). We assume the c_n to be uncorrelated with zero mean value

$$\left\langle c_n c_m^* \right\rangle = \left\langle c_n \right\rangle\left\langle c_m^* \right\rangle = 0\,, \qquad (n \neq m)\,, \tag{5.2.7}$$

whereas their mean squared modulus equals the eigenvalues

$$\left\langle |c_n|^2 \right\rangle = \eta_n\,, \qquad (n = 0,1,....)\,. \tag{5.2.8}$$

Equations (5.2.7) and (5.2.8) can be synthesized by the single equation

$$\left\langle c_n c_m^* \right\rangle = \eta_n\delta_{nm}\,, \qquad (n,m = 0,1,....)\,. \tag{5.2.9}$$

We now compute the correlation function for U at two points $\mathbf{r}_1$ ed $\mathbf{r}_2$ for zero delay

$$\left\langle U(\mathbf{r}_1,t)U^*(\mathbf{r}_2,t)\right\rangle = \sum_{n=0}^{\infty}\sum_{m=0}^{\infty}\left\langle c_n c_m^*\right\rangle \Phi_n(\mathbf{r}_1)\Phi_m^*(\mathbf{r}_2) = \sum_{n=0}^{\infty}\eta_n\Phi_n(\mathbf{r}_1)\Phi_n^*(\mathbf{r}_2)\,, \qquad (5.2.10)$$

where eqs. (5.2.6) and (5.2.9) have been used. On comparing eq. (5.2.4) and (5.2.10) we derive the equality

$$W(\mathbf{r}_1,\mathbf{r}_2) = \left\langle U(\mathbf{r}_1,t)U^*(\mathbf{r}_2,t)\right\rangle . \qquad (5.2.11)$$

Let us briefly discuss the meaning of this result. According to eq. (5.2.11), the cross spectral density, at each frequency ν, can be thought of as the ensemble correlation function for zero delay of a suitable monochromatic field obtained by the superposition (5.2.6) under the constrain (5.2.9). While the field is perfectly coherent in each realization because it is monochromatic, coherence is generally reduced by the average operation (5.2.10). There is only one case in which coherence is retained. This is when only one of the eigenvalues, say the m-th one, is different from zero. Equation (5.2.4) then becomes

$$W(\mathbf{r}_1,\mathbf{r}_2) = \eta_m\Phi_m(\mathbf{r}_1)\,\Phi_m^*(\mathbf{r}_2)\,, \qquad (5.2.12)$$

and the degree of spatial coherence is

$$\mu(\mathbf{r}_1,\mathbf{r}_2) = \frac{\eta_m\Phi_m(\mathbf{r}_1)\,\Phi_m^*(\mathbf{r}_2)}{\left[\eta_m^2\,|\Phi_m(\mathbf{r}_1)|^2\,|\Phi_m(\mathbf{r}_2)|^2\right]^{1/2}} = e^{i[\alpha_m(\mathbf{r}_1)-\alpha_m(\mathbf{r}_2)]}\,, \qquad (5.2.13)$$

where $\alpha_m(\mathbf{r})$ is the argument of $\Phi_m(\mathbf{r})$. It is apparent that the modulus of μ is one so that the field is completely coherent.

Both the functions $\Psi_m(\mathbf{r},t)$ and their spatial part $\Phi_m(\mathbf{r})$, are known as the modes of the partially coherent source and this is why the above outlined theory is often quoted as the modal theory of coherence. An alternative name is coherence theory in the space-frequency domain. Note that the analytic form of the modes can change with frequency because the kernel of eq. (5.2.1), i. e., the cross spectral density, is a function of frequency. The same occurs for the eigenvalues.

Let us illustrate the meaning of the eigenvalues. Define the integrated spectral density as

$$P(\nu) = \int_S G(\mathbf{r},\nu)\,d^2r\,. \qquad (5.2.14)$$

The quantity P(ν) is a measure of the overall power emitted at frequency ν by the source. On inserting eq. (5.2.4) written with $\mathbf{r}_1=\mathbf{r}_2=\mathbf{r}$ into eq. (5.2.14) and using eq. (5.2.3), we easily find

$$P(\nu) = \sum_{n=0}^{\infty}\eta_n\,. \qquad (5.2.15)$$

Therefore, the typical eigenvalue η_n can be interpreted as the contribution from the n-th mode to the integrated spectral density.

Generally speaking the modes of a partially coherent source are difficult to find in that the integral equation (5.2.1) has to be solved. Although for a number of sources the explicit form of the modes has been found the search is continuing. To this aim certain formal analogies with problems of quantum mechanics can be exploited. An elegant example of this has been offered in ref. 43 where the modes of a generalized version of the Collett-Wolf source known as twisted Gaussian Schell-model source were evaluated.

In spite of the above mentioned difficulty, the modal theory affords a powerful tool for understanding many aspects of coherence theory and has proved its usefulness in several problems.

5.3) An example

In this section, we shall give an explicit example of modal expansion. First, however, we discuss a pair of models of partially coherent sources.

A source is said to be of the Schell-model type if its cross spectral density has the form

$$W(\mathbf{r}_1,\mathbf{r}_2) = \sqrt{G(\mathbf{r}_1)G(\mathbf{r}_2)}\;\mu(\mathbf{r}_1-\mathbf{r}_2)\,. \qquad (5.3.1)$$

The essential point is that the degree of spectral coherence depends on $\mathbf{r}_1$ and $\mathbf{r}_2$ only through their difference. Once this condition is satisfied, eq. (5.3.1) follows from eq. (5.1.3). Sources of the Schell-model type play an important role in coherence theory and are easily synthesized in the laboratory. We omitted again the explicit dependence on ν because we are going to work at a single frequency. It should be appreciated however that the ν-dependence is implicit. This means for example that for a given source $\mu(\mathbf{r}_1-\mathbf{r}_2)$ can be a different function of $\mathbf{r}_1-\mathbf{r}_2$ at different frequencies.

For a large class of sources, the degree of spectral coherence is a function of $\mathbf{r}_1-\mathbf{r}_2$ that decreases quite rapidly as compared to the law of variation of $G(\mathbf{r})$ with respect to $\mathbf{r}$. To a good approximation, the cross spectral density for such sources can be written

$$W(\mathbf{r}_1,\mathbf{r}_2) = G\left(\frac{\mathbf{r}_1+\mathbf{r}_2}{2}\right)\mu(\mathbf{r}_1-\mathbf{r}_2)\,. \qquad (5.3.2)$$

Sources of this class are known as quasi homogeneous [10] [a strictly homogeneous source would be one for which $W(\mathbf{r}_1,\mathbf{r}_2)=W(\mathbf{r}_1-\mathbf{r}_2)$]. They furnish a very good description of many natural sources. Their analytical form simplifies several problems [10].

After these preliminaries, let us consider the so-called Collett-Wolf source [11,12] or Gaussian Schell-model source. Its cross spectral density is

$$W(\mathbf{r}_1,\mathbf{r}_2) = G_0\, e^{-\frac{r_1^2+r_2^2}{4\sigma_G^2}}\, e^{-\frac{(\mathbf{r}_1-\mathbf{r}_2)^2}{2\sigma_\mu^2}}\,, \qquad (5.3.3)$$

for each temporal frequency. On the other hand, the parameters G_o, σ_G and σ_μ generally depend on the frequency. The spectral density and the degree of coherence are given by

$$G(\mathbf{r}) = G_0\, e^{-\frac{r^2}{2\sigma_G^2}}\,; \qquad \mu(\mathbf{r}_1-\mathbf{r}_2) = e^{-\frac{(\mathbf{r}_1-\mathbf{r}_2)^2}{2\sigma_\mu^2}}\,. \qquad (5.3.4)$$

At any frequency, the source has the form of a gaussian disc and, in the neighbourhood of any point, the coherence area is a gaussian disc too. The parameters σ_G and σ_μ can be taken as equivalent radii of the source and the coherence area respectively. Note that the ratio σ_μ/σ_G can be chosen arbitrarily. As a consequence, the coherence features can be very different passing from a globally incoherent source for $\sigma_\mu << \sigma_G$ to a nearly completely coherent one for $\sigma_\mu >> \sigma_G$. In particular, for $\sigma_\mu << \sigma_G$ eq. (5.3.3) can be easily given the form (5.3.2).

The Collett-Wolf source was very important in clarifying the relationship between directionality and spatial coherence and, more generally, between coherence and radiometry. It was shown, in fact that such a source even in the quasi-homogeneous limit could generate the same far zone intensity distribution as a laser. This came as a surprise inasmuch as the high directionality of a laser beam was traditionally attributed to its full spatial coherence. This prediction, which was confirmed by experiments [17,18], stimulated a large number of investigations with many significant results [19-40].

In view of the importance of this type of source, it is interesting to find the corresponding modal structure. If the kernel (5.3.3) is inserted into eq. (5.2.1), the following eigenfunctions and eigenvalues are found [22,23]

$$\Phi_{mn}(x,y) = \frac{1}{v_o}\sqrt{\frac{2}{\pi 2^{m+n} m!n!}}\, H_m\left(\frac{x\sqrt{2}}{v_o}\right) H_n\left(\frac{y\sqrt{2}}{v_o}\right) e^{-\frac{x^2+y^2}{v_o^2}}\,; \qquad (5.3.5)$$

$$\eta_{mn} = \eta_0 q^{m+n}; \qquad (m,n = 0,1,.....)\,, \qquad (5.3.6)$$

where the parameters v_o, η_o and q are given by

$$\frac{1}{v_o^2} = \frac{1}{4\sigma_G^2}\sqrt{1+\left(\frac{2\sigma_G}{\sigma_\mu}\right)^2}\,; \qquad (5.3.7)$$

$$\eta_o = \frac{8\pi G_o \sigma_G^2}{\left[1+\sqrt{1+\left(\frac{2\sigma_G}{\sigma_\mu}\right)^2}\right]^2}\,; \qquad (5.3.8)$$

$$q = \frac{\left(2\sigma_G/\sigma_\mu\right)^2}{\left[1+\sqrt{1+\left(\frac{2\sigma_G}{\sigma_\mu}\right)^2}\right]^2}\,. \qquad (5.3.9)$$

In eqs. (5.3.5) and (5.3.6) a double index has been used instead if the single one appearing in section 5.2. This gives a simpler ordering of eigenfunctions and eigenvalues. In addition, cartesian coordinates have replaced position vectors.

The form of the modes is well familiar. Equation (5.3.5) gives in fact the field distribution across the waist of the Hermite-Gauss modes of laser theory [44]. It is seen from eq. (5.3.6) that the eigenvalues decrease according to a geometrical progression. We could define an equivalent number of modes by taking into account only those modes whose eigenvalues are appreciably different from zero. Then, it would be found that the equivalent number of modes is an increasing function of σ_G/σ_μ. In other words, poorly coherent sources have a large equivalent number of modes.

5.4) Propagation of partially coherent fields

Upon propagation partially coherent fields can exhibit behaviors that are rather different from those pertaining to coherent fields. In order to show this we shall first refer to

the simple case of paraxial propagation. As we said at the end of section 5.1, we can use eq. (2.1.11) with J replaced by W. More explicitly, we have

$$W(\mathbf{r}_1,\mathbf{r}_2,\nu)=\frac{\nu^2}{c^2z^2}\iint W_o(\boldsymbol{\rho}_1,\boldsymbol{\rho}_2,\nu)e^{\frac{i\pi\nu}{cz}\left[(\mathbf{r}_1-\boldsymbol{\rho}_1)^2-(\mathbf{r}_2-\boldsymbol{\rho}_2)^2\right]}d^2\rho_1 d^2\rho_2 . \qquad (5.4.1)$$

Here, c is the speed of light and both λ and k are expressed through ν. The spectral density is obtained by letting $\mathbf{r}_1=\mathbf{r}_2$. Accordingly,

$$G(\mathbf{r},\nu)=\frac{\nu^2}{c^2z^2}\iint W_o(\boldsymbol{\rho}_1,\boldsymbol{\rho}_2,\nu)e^{\frac{i\pi\nu}{cz}\left[\rho_1^2-\rho_2^2-2\mathbf{r}\cdot(\boldsymbol{\rho}_1-\boldsymbol{\rho}_2)\right]}d^2\rho_1 d^2\rho_2 . \qquad (5.4.2)$$

We see from eq. (5.4.2) that the spectral density at $\mathbf{r}$ depends on the field correlation properties across the plane z=0. To have a clearer insight, let us use eq. (5.1.3) into eq. (5.4.2). This gives

$$G(\mathbf{r},\nu)=$$
$$\frac{\nu^2}{c^2z^2}\iint\sqrt{G_o(\boldsymbol{\rho}_1,\nu)G_o(\boldsymbol{\rho}_2,\nu)}\mu_o(\boldsymbol{\rho}_1,\boldsymbol{\rho}_2,\nu)e^{\frac{i\pi\nu}{cz}\left[\rho_1^2-\rho_2^2-2\mathbf{r}\cdot(\boldsymbol{\rho}_1-\boldsymbol{\rho}_2)\right]}d^2\rho_1 d^2\rho_2 . \qquad (5.4.3)$$

Equation (5.4.3) makes it clear that even for a prescribed form of $G_o(\boldsymbol{\rho},\nu)$ the spectral density can be different for sources characterized by distinct degrees of coherence. In order to see some implications of this result we shall first refer to the case in which only a single frequency is considered leaving the general case for the next section. According to the terminology discussed in Section 4.1 we shall speak of G as the optical intensity.

A case that received much attention [11, 12, 17-40] is the propagation of the field generated by the Collett-Wolf source. The corresponding spatial intensity distribution can be obtained on inserting eq. (5.3.3) into eq. (5.4.2) and evaluating the resulting integral. We shall adopt however a different approach based on the modal expansion because this leads to a very simple picture of the propagation process. We have seen that the modes in Section 5.3 that the modes pertaining to the Collett-Wolf source are Hermite -Gauss modes. As is well known from laser cavity theory [44] each of them propagates according to the simple law

$$\Phi_{mn}(x,y,z)=\frac{1}{v(z)}\sqrt{\frac{2}{\pi 2^{m+n}m!n!}}\times$$
$$\times e^{i[kz-(n+m+1)\Psi(z)]}H_m\left(\frac{x\sqrt{2}}{v(z)}\right)H_n\left(\frac{y\sqrt{2}}{v(z)}\right)e^{\left(\frac{ik}{2R(z)}-\frac{1}{v^2(z)}\right)(x^2+y^2)} . \qquad (5.4.4)$$

where

$$R(z)=z\left[1+\left(\frac{\pi v_o^2}{\lambda z}\right)^2\right];\ v^2(z)=v_o^2\left[1+\left(\frac{\lambda z}{\pi v_o^2}\right)^2\right];\quad \Psi(z)=\operatorname{arctg}\left(\frac{\lambda z}{\pi v_o^2}\right). \qquad (5.4.5)$$

Taking the squared modulus of eq. (5.4.5) we see that the intensity distribution of each mode maintains the same shape across any plane z=const. The only change is a pattern magnification by a factor $v(z)/v_0$ Now, according to the modal theory the overall field produced by the partially coherent source is a superposition of mutually uncorrelated modes. As a consequence, the total intensity is simply the sum of the intensities pertaining to the various modes each of them being weighted by the corresponding eigenvalue. This can be seen from eq. (5.2.4) letting $\mathbf{r}_1=\mathbf{r}_2$. We conclude that the optical intensity distribution is shape invariant the only effect of propagation being a transverse scale magnification. It may be worthwhile to note that this would not be the case were the superposition of coherent type. As shown by eq. (5.4.4) in fact modes with different values of n+m experience different phase shifts on propagation. Therefore in a coherent superposition the interference pattern among the various modes would change from one plane to another.

The previous shape invariant propagation of the beam generated by a Collett-Wolf source can be seen as a sort of generalization of the properties of a single Hermite-Gauss coherent beam.Thus it may be helpful to show a case in which a partially coherent beam has propagation features that could not be attained with a coherent beam. Instead of eq. (5.3.3) let us consider the following slightly different form [29] for the cross spectral density across the plane z=0

$$W(x_1,y_1,x_2,y_2)=G_o e^{-\frac{x_1^2+x_2^2}{4\sigma_{Gx}^2}}e^{-\frac{y_1^2+y_2^2}{4\sigma_{Gy}^2}}e^{-\frac{(x_1-x_2)^2}{2\sigma_{\mu x}^2}}e^{-\frac{(y_1-y_2)^2}{2\sigma_{\mu y}^2}} . \qquad (5.4.6)$$

Again both the intensity and the degree of coherence across the source are Gaussianly shaped. Yet there can be an anisotropy between x and y if the intensity and coherence variances along the two axes are different. Generally speaking the beam generated by such a source will not be shape invariant. However the shape invariance holds if the following condition is met [29]

$$\frac{1}{\left(\sigma_{Gx}^2\right)}\left(\frac{1}{4\sigma_{Gx}^2}+\frac{1}{\sigma_{\mu x}^2}\right)=\frac{1}{\left(\sigma_{Gy}^2\right)}\left(\frac{1}{4\sigma_{Gy}^2}+\frac{1}{\sigma_{\mu y}^2}\right). \qquad (5.4.7)$$

This condition can be satisfied by beams whose cross section is shaped in the form of thin, elongated ellipses. In this case the beam appears as a sort of luminous blade. This is why these fields are known as blade-like. No similar behaviour could be obtained by a coherent beam. As a matter of fact if we start from an elliptical coherent field distribution elongated along say the x-axis the very law of diffraction makes it change into an ellipse rotated by 90° in the course of propagation as is well known from the study of astigmatic beams.

There is another aspect relating to propagation phenomena that we can briefly treat. We noted already that a partially coherent field possesses a huge quantity of information. To specify in a complete way a partially coherent field we have to give the cross spectral density for each frequency and at any pair of points across a selected plane. Direct and inverse propagation formulas can then be used to evaluate the cross spectral density at any other pair of points in space. Simple as this may be at the analytical level, it takes an enormous effort if the characterization is to be done experimentally. We should manage in fact a five dimensional set of data. In addition, the measurement of the cross spectral density, although straightforward in principle, is an error prone and time consuming process A much simpler task is to measure the intensity (at any selected frequency) even across a multitude of planes. One is therefore led to ask what kind of information about the field can be deduced by knowledge of the intensity alone. Could perhaps the complete intensity distribution in space be enough to determine the cross spectral density at a certain plane (hence everywhere thanks to propagation formulas)? Let us put it another way. Can two wavefields with different coherence properties give rise to the same intensity everywhere? There is a tendency to assume that the answer is negative and that the space intensity distribution of a field gives a sufficient characterization of it. Indeed this is tacitly assumed whenever we characterize laser beam by some global parameter such as the M^2-factor related to its space intensity distribution. Yet the answer to the above question is positive. There exist fields endowed with different coherence properties that cannot be distinguished on an intensity base only. We shall show this by a simple example.

Let us consider the following monochromatic field distributions

$$V^{\pm}(r,\vartheta,z) = A\, e^{i[kz-2\Psi(z)]}\, \frac{r v_0 \sqrt{2}}{v^2(z)}\, e^{\left[\frac{ik}{2R(z)} - \frac{1}{v^2(z)}\right] r^2}\, e^{\pm i\vartheta}\,, \tag{5.4.8}$$

where $v(z)$, $R(z)$, and $\Psi(z)$ are given by eq.(5.4.5). For either choice of the sign eq. (5.4.8) represents a simple Laguerre-Gauss laser mode [44]. Clearly, the corresponding intensity distribution is the same regardless of the sign we choose. We have here two coherent wavefields producing the same intensity everywhere. Suppose now that we construct an ensemble of fields of the form

$$V(r,\vartheta,z) = a^{+}V^{+}(r,\vartheta,z) + a^{-}V^{-}(r,\vartheta,z)\,, \tag{5.4.9}$$

where a^+ and a^- are uncorrelated random coefficients with zero mean and the following mean squared values

$$\left\langle \left|a^{+}\right|^2 \right\rangle = \left\langle \left|a^{-}\right|^2 \right\rangle = \frac{1}{2}\,. \tag{5.4.10}$$

It is easily seen that the field (5.4.9) gives everywhere the same intensity that would be produced by either V^+ or V^-. Yet, the field (5.4.9) is partially coherent. It is not difficult to evaluate the modulus of the pertaining degree of coherence. This turns out to be

$$\left|\mu\left(r_1,\vartheta_1,z;r_2,\vartheta_2,z\right)\right| = \left|\cos\left(\vartheta_1 - \vartheta_2\right)\right|\,. \tag{5.4.11}$$

Although the field (5.4.9) is indistinguishable from the coherent field V^+ or V^- on an intensity basis, it has different physical properties. It is to be stressed that such different properties would be revealed by most interference or diffraction experiments.

The existence of fields with different states of coherence yet producing the same intensity everywhere does not mean, of course, that the intensity distribution is an irrelevant constraint as far as the determination of a partially coherent field is concerned. However, the exact influence of this constraint is still under investigation [41, 42].

5.5) Spectral changes induced by source correlations

The words "spectrum of a light field" are often used as if they were of unambiguous meaning. The phrases "spectrum of a star", "spectrum of a lamp" are example of this usage. To be more precise we introduce the so-called normalized spectrum of a radiation field defined as follows

$$S(P,\nu) = \frac{G(P,\nu)}{\int_0^{\infty} G(P,\nu)d\nu}\,. \tag{5.5.1}$$

It is a widely held idea that the normalized spectrum is uniquely determined by the spectrum of the source fluctuations and that it is independent of the observation point. Except for some pioneering papers in [2,7] such an idea was not questioned until relatively recent times [31, 45] . Since then a great deal of research has been carried out stimulated by the results of

Wolf [45-61]. In order to show that the above idea is generally incorrect we shall refer to a very simple example first proposed by Wolf [48]. Let us consider two very small sources located at certain points A_1 and A_2. The field produced by these sources at point P and frequency ν can be written

$$U(P,\nu) = Q_1(\nu)\frac{e^{ikR_1}}{R_1} + Q_2(\nu)\frac{e^{ikR_2}}{R_2}, \qquad (5.5.2)$$

where $R_1(R_2)$ is the distance between P and $A_1(A_2)$ while Q_1 and Q_2 denote the source fluctuations (e.g., charge density). On multiplying eq.(5.5.2) by its complex conjugate and taking an ensemble average we obtain the following expression for the spectrum at P

$$G(P,\nu) = \frac{\langle |Q_1(\nu)|^2 \rangle}{R_1^2} + \frac{\langle |Q_2(\nu)|^2 \rangle}{R_2^2} + 2\frac{\mathrm{Re}\left\{\langle Q_1(\nu)Q_2^*(\nu)\rangle e^{ik(R_1-R_2)}\right\}}{R_1R_2}. \qquad (5.5.3)$$

For the sake of simplicity we assume the source spectrum to be the same at A_1 and A_2. Letting

$$G_Q(\nu) = \langle |Q_1(\nu)|^2 \rangle = \langle |Q_2(\nu)|^2 \rangle; \qquad W_{12}(\nu) = \langle Q_1(\nu)Q_2^*(\nu)\rangle, \qquad (5.5.4)$$

eq.(5.5.3) becomes

$$G(P,\nu) = G_Q(\nu)\left(\frac{1}{R_1^2} + \frac{1}{R_2^2}\right) + 2\frac{\mathrm{Re}\left\{W_{12}(\nu)e^{ik(R_1-R_2)}\right\}}{R_1R_2}. \qquad (5.5.5)$$

Here we see that the field spectrum G(P, ν) depends not only on the source spectrum $G_a(\nu)$ but also on the correlation function W_{12} between the source fluctuations. Equation (5.5.5) is formally identical to the familiar law describing two wave interference. Yet while the ordinary interference formula accounts for spatial variations of the optical intensity here the observation point has been fixed and we inquire about the dependence on ν of the spectral density G(P, ν). Wolf showed that different spectra can be obtained at a fixed observation point for different source correlation laws. These predictions were confirmed by experimental results [49, 51].

Two essential conclusions should be suggested by the above example: a) source correlations affect the field spectrum; b) the normalized field spectrum may change in space.

Although the previous conclusions are sound we may wonder why these types of phenomena were not observed before. As shown by eq.(5.5.5) for the case $W_{12}(\nu) \equiv 0$ a possible answer is that no spectral modification is to be expected if the source is strictly

incoherent in the sense that no correlation exists between any two source elements. Such a crude model for a natural source however is rather unphysical in that it is known that source correlations exist across regions where linear dimensions are at least of the order of the wavelength. One is then led to inquire about the existence of correlated sources that can produce the same normalized spectrum at any observation point. In this connection an important result was obtained by Wolf [45]. He considered a planar source of the quasi-homogeneous kind (see eq.(5.3.2)) and confined attention to the far-zone. On assuming that the fluctuation spectrum was the same across the whole source, Wolf showed that the normalized far-zone field spectrum in a direction specified by the unit vector **u** had the following expression

$$S^{\infty}(\mathbf{u},\nu) = \frac{k^2G_0(\nu)\tilde{\mu}_0(k\mathbf{u}_p,\nu)}{\int_0^{\infty} k^2G_0(\nu)\tilde{\mu}_0(k\mathbf{u}_p,\nu)d\nu}. \qquad (5.5.6)$$

Here G_0 is the field spectrum at the source plane, μ_0 is the corresponding degree of coherence and the tilde denotes the Fourier transform. Furthermore, $\mathbf{u}_P$ is the vector obtained by projection of $\underline{u}$ on the source plane.

It is easily seen that the normalized far-zone spectrum is generally different from the normalized spectrum at the source because of a) the factor k_2; b) the factor $\tilde{\mu}_0$. Suppose however that μ_0 has the following form

$$\mu_0(\boldsymbol{\rho}_1 - \boldsymbol{\rho}_2) = h\left[k(\boldsymbol{\rho}_1 - \boldsymbol{\rho}_2)\right], \qquad (5.5.7)$$

where h is any correlation function such that h(0)=1. On computing the Fourier transform $\tilde{\mu}_0$ we obtain

$$\tilde{\mu}_0(k\mathbf{u}_p,\nu) = \frac{1}{(2\pi)^2}\int \mu_0(\boldsymbol{\rho}')\, e^{ik\mathbf{u}_p\cdot\boldsymbol{\rho}'}d^2\rho' = \frac{1}{(2\pi k)^2}\int h(\boldsymbol{\sigma})\, e^{i\mathbf{u}_p\cdot\boldsymbol{\sigma}}d^2\sigma = \tilde{h}(\mathbf{u}_p), \qquad (5.5.8)$$

where we let $\boldsymbol{\rho}_1 - \boldsymbol{\rho}_2 = \boldsymbol{\rho}'$ and $k\boldsymbol{\rho}' = \boldsymbol{\sigma}$. On inserting eq.(5.5.8) into eq. (5.5.6) we have

$$S^{\infty}(\mathbf{u},\nu) = \frac{G_0(\nu)}{\int_0^{\infty} G_0(\nu)d\nu}. \qquad (5.5.9)$$

The far-zone normalized spectrum is now independent of the observation point. In addition, it equals the normalized spectrum at the source plane. Accordingly, eq.(5.5.7) is a sufficient condition for a quasi-homogeneous source to produce throughout the far zone the same

normalized spectrum as at the source plane. This beautifully simple result is known as the Wolf's scaling law.

An important class of sources obeying the scaling law is given by the Lambertian sources so that eq.(5.5.7) is likely to apply to several natural sources. However when the degree of coherence violates the scaling law the spectral invariance is generally lost. This was first proved experimentally by Morris and Faklis [50].

Other experiments were performed by Indebetouw [52] and by Kandpal, Vaishya and Joshi [53]. The latter authors also made some important work [54, 55] about the implications of the Wolf's effect on the spectroradiometric scales. Such scales are maintained by the national standard laboratories of the various countries. Comparison among radiometric scales from different laboratories revealed large differences. The work by Kandpal, Vaishya and Joshi suggests that some of these discrepancies could be caused by the Wolf's effect.

We also mention that spectral changes rather similar to the ones produced by source correlations can be exhibited in scattering phenomena [56, 57].

A good review paper about spectral changes due to source correlations is ref. 62.

5.6) A glance at further topics of coherence theory

The aim of this final section is to sketch very briefly a few other topics of current interest in coherence theory.

One of them can be traced back to a question first raised by Wolf [62]. Why is laser light (generally) coherent? It can be crudely said that the laser cavity selects a single mode, which is a coherent field. However, a description based on the exact laws of coherence evolution is much richer than that [64-70]. The fundamental phenomenon is propagation of partially coherent light through periodic sequences of apertures and lenses. It has been shown recently that in certain cases partially coherent modes exist [69]. In addition, some lasers produce very short pulses so that their emission cannot be described by a stationary state. The study of coherence of transient states then becomes essential.

Speaking of periodic structures we may add that there is a connection between this subject and the one dealing with transversally periodic objects illuminated by partially coherent light. This is another area of current interest [71, 72].

We finally point out the investigations about formal analogies between classical coherence theory and quantum mechanics. To avoid misunderstanding, we stress that we are not alluding to the quantum theory of coherence. We are simply saying that certain tools of coherence theory are mathematically equivalent to well known quantities of quantum

mechanics. The most significant of these correspondences is between the cross spectral density of coherence theory and the coordinate representation of quantum mechanics. As a consequence, known results from one field can be transferred to the other. The reader can consult refs. 43 and 73 for beatiful examples of this.

The list of themes and references given in the present notes is far from being complete but it should give an idea of the vastity of coherence phenomena.

REFERENCES

1) M. Born and E. Wolf, Principles of Optics, New York: Pergamon Press, 1980
2) L. Mandel, E. Wolf, Rev.Mod.Phys., **37**, (1965) 231
3) J. W. Goodman, Statistical Optics, Wiley, New York, 1985
4) G. A. Vanasse, H.Sakai, "Fourier Spectroscopy" in: Progress in Optics, Ed.E.Wolf, Vol. VI, pp. 261-330, North-Holland, Amsterdam, 1967
5) R. Hanbury Brown and R. Q. Twiss, Nature, **177** (1956) 27
6) T. W. Cole, "Quasi-Optical Techniques of Radio-Astronomy", in Progress in Optics, Ed.E.Wolf, Vol. XV, pp. 187-244, North-Holland, Amsterdam, 1977
7) L. Mandel, E. Wolf, J. Opt. Soc. Am., **66** (1976) 529
8) E. Wolf, J. Opt. Soc. Am., **72**, (1982) 343
9) E. Wolf, J. Opt. Soc. Am. A, **3**, (1986) 76
10) W. H. Carter and E. Wolf, J. Opt. Soc. Am., **67** (1977) 785
11) E. Collett and E. Wolf, Opt. Lett., **2** (1978) 27
12) E. Wolf and E. Collett, Opt. Comm., **25** (1978) 293
13) A. Walther, J. Opt. Soc. Am., **58** (1968) 1256
14) A. Walther, J. Opt. Soc. Am., **63** (1973) 1622
15) E. W. Marchand and E. Wolf, J. Opt. Soc. Am., **64** (1974) 1219
16) E. Wolf, J. Opt. Soc. Am., **68** (1978) 6
17) P. De Santis, F. Gori, G. Guattari and C. Palma, Opt. Comm., **28** (1979) 256
18) J. D. Farina, L. M. Narducci and E. Collett, Opt. Comm., **32** (1980) 203
19) J. T. Foley and M. S. Zubairy, Opt. Comm., **26** (1978) 297
20) F. Gori and C. Palma, Opt. Comm., **27** (1978) 185
21) B. E. A. Saleh, Opt. Comm., **30** (1979) 135
22) F. Gori, Opt. Comm., **34** (1980) 301
23) A. Starikov and E. Wolf, J. Opt. Soc. Am., **72** (1982) 923
24) A. T. Friberg and R. J. Sudol, Opt. Comm., **41** (1982) 383
25) A. T. Friberg, Opt. Eng., **21** (1982) 927

26) Y. Li and E. Wolf, Opt. Lett., **7** (1982) 256
27) F. Gori, Opt. Comm., **46** (1983) 149
28) A. T. Friberg and R. J. Sudol, Optica Acta, **30** (1983) 1075
29) F. Gori and G. Guattari, Opt. Comm., **48** (1983) 7
30) R. Simon, E. G. C. Sudarshan and N. Mukunda, Phys. Rev. A, **29** (1984) 2373
31) F. Gori and R. Grella, Opt.Comm., **49** (1984) 173
32) R. Simon, E. G. C. Sudarshan and N. Mukunda, Phys. Rev. A, **31** (1985) 2414
33) A. T. Friberg and J.Turunen, Opt. and Lasers Tech., **25** (1986) 857
34) M. Nieto-Vesperinas, J. Opt. Soc. Am. A, **3** (1986) 1354
35) A. Gamliel, Opt. Comm., **60** (1986) 333
36) M. Zahid and M. S .Zubairy, Opt. Comm., **64** (1987) 496
37) A. T. Friberg and J. Turunen, J. Opt. Soc. Am. A, **5** (1988) 713
38) R. Simon, N. Mukunda and E. C. G. Sudarshan, Opt.Comm., **65** (1988) 322
39) J. Turunen, A. Vasara and A. T. Friberg, J.Opt.Soc.Am. A, **8** (1991) 282
40) R. Martinez-Herrero and P. M. Mejias, Opt. Comm., **94** (1992) 197
41) F. Gori, M. Santarsiero and G. Guattari, J. Opt. Soc. Am. A, **10** (1993) 673
42) V. Bagini, F. Gori, M. Santarsiero, G. Guattari and G. Schirripa Spagnolo, Opt. Comm., **102** (1993) 495
43) R. Simon and N. Mukunda, J. Opt. Soc. Am. A, **10** (1993) 95
44) A. E. Siegman, Lasers, University Science Books, Mill Valley, 1986
45) E. Wolf, Phys. Rev. Lett., **56** (1986) 1370
46) E. Wolf, Nature, **326** (1987) 363
47) E. Wolf, Opt.Comm., **62** (1987) 12
48) E. Wolf, Phys. Rev. Lett., **58** (1987) 2646
49) M. F. Bocko, D. H. Douglass and R. S. Knox, Phys. Rev. Lett., **58** (1987) 2649
50) G. M. Morris and D. Faklis, Opt.Comm., **62** (1987) 5
51) F. Gori, G. Guattari C. Palma and C. Padovani, Opt. Comm., **67** (1988) 1
52) G. Indebetow, J. Mod. Opt., **36** (1989) 251
53) H. C. Kandpal, J. S. Vaishya and K. C. Joshi, Phys. Rev. A., **41** (1990) 4541
54) H. C. Kandpal, J. S. Vaishya and K. C. Joshi, Opt. Comm., **73** (1989) 169
55) K. C. Joshi, H. C. Kandpal and J. S. Vaishya, Appl. Opt., **30** (1991) 1471
56) E. Wolf, J. T. Foley and F. Gori, J. Opt. Soc. Am. A, **6** (1989) 1142
57) J . T. Foley and E. Wolf , Phys. Rev. A, **40** (1989) 588
58) K. E. Drake, G. Cuossen, D. A. Wiersma, H. A. Ferwerda and B. J. Hoenders,Phys. Rev. Lett., **65** (1990) 1427
59) A. Lagendijk, Phys.Lett. A ,**147** (1990) 389
60) F. Gori, G. L. Marcopoli and M. Santarsiero, Opt. Comm., **81** (1991) 123
61) K. A. Nugent, Opt.Comm., **91** (1992) 13

62) H. C. Kandpal, J. S. Vaishya and K. C. Joshi, Opt. Engineering, **33** (1994) 1996
63) E. Wolf, Phys.Lett.,**3** (1963) 166
64) W. Streifer, J. Opt. Soc. Am. **56** (1966) 1481
65) F. Gori, Atti Fond. Giorgio Ronchi **35** (1980) 434
66) E. Wolf and G. S. Agarwal, J. Opt. Soc. Am. A, **1** (1984) 541
67) T. Shirai and T. Asakura, Optik **94** (1993) 123
68) T. Shirai and T. Asakura, J. Opt. Soc. Am. A, **11** (1994) 1141
69) A. Friberg and J. Turunen, J. Opt. Soc. Am. A, **11** (1994) 227
70) G. Cincotti, P. De Santis, G. Guattari and C. Palma, Pure and Appl. Opt. **3** (1994) 561
71) K. Patorski, in Progress in Optics, E. Wolf ed. (Elsevier, Amsterdam, 1989) Vol 27
72) H. Yoshimura, N. Takai and T. Asakura, J. Opt. Soc. Am. A, **11** (1994) 2112
73) R. Gase, J. Opt. Soc. Am. A, **11** (1994) 2121